Journal of Biomechanics 47 (2014) 3882–3890

Contents lists available at ScienceDirect

Journal of Biomechanics

journal homepage: www.elsevier.com/locate/jbiomech
www.JBiomech.com

The effect of inlet waveforms on computational hemodynamics of patient-specific intracranial aneurysms

J. Xiang [a,b,c], A.H. Siddiqui [a,c,d], H. Meng [a,b,c,e,*]

[a] Toshiba Stroke and Vascular Research Center, University at Buffalo, State University of New York, Buffalo, NY 14203, USA
[b] Department of Mechanical and Aerospace Engineering, University at Buffalo, State University of New York, Buffalo, NY 14260, USA
[c] Department of Neurosurgery, University at Buffalo, State University of New York, Buffalo, NY 14203, USA
[d] Department of Radiology, University at Buffalo, State University of New York, Buffalo, NY 14203, USA
[e] Department of Biomedical Engineering, University at Buffalo, State University of New York, Buffalo, NY 14260, USA

ARTICLE INFO

Article history:
Accepted 29 September 2014

Keywords:
Intracranial aneurysm
Computational flow dynamics
Boundary condition
Inlet waveform
Wall shear stress
Oscillatory shear index

ABSTRACT

Due to the lack of patient-specific inlet flow waveform measurements, most computational fluid dynamics (CFD) simulations of intracranial aneurysms usually employ waveforms that are not patient-specific as inlet boundary conditions for the computational model. The current study examined how this assumption affects the predicted hemodynamics in patient-specific aneurysm geometries. We examined wall shear stress (WSS) and oscillatory shear index (OSI), the two most widely studied hemodynamic quantities that have been shown to predict aneurysm rupture, as well as maximal WSS (MWSS), energy loss (EL) and pressure loss coefficient (PLc). Sixteen pulsatile CFD simulations were carried out on four typical saccular aneurysms using 4 different waveforms and an identical inflow rate as inlet boundary conditions. Our results demonstrated that under the same mean inflow rate, different waveforms produced almost identical WSS distributions and WSS magnitudes, similar OSI distributions but drastically different OSI magnitudes. The OSI magnitude is correlated with the pulsatility index of the waveform. Furthermore, there is a linear relationship between aneurysm-averaged OSI values calculated from one waveform and those calculated from another waveform. In addition, different waveforms produced similar MWSS, EL and PLc in each aneurysm. In conclusion, inlet waveform has minimal effects on WSS, OSI distribution, MWSS, EL and PLc and a strong effect on OSI magnitude, but aneurysm-averaged OSI from different waveforms has a strong linear correlation with each other across different aneurysms, indicating that for the same aneurysm cohort, different waveforms can consistently stratify (rank) OSI of aneurysms.

1. Introduction

Intracranial aneurysms (IAs) are pathological dilatations of arterial walls that affect up to 5% of the entire population (Rinkel et al., 1998). Ruptured IAs cause subarachnoid hemorrhage and its sequelae, resulting in significant morbidity and mortality (Broderick et al., 1994; Cross et al., 2003; Hop et al., 1997). Image-based computational fluid dynamics (CFD) has been widely used to obtain patient-specific hemodynamic fields in IAs to stratify aneurysm rupture risk (Cebral et al., 2011; Jou et al., 2008; Meng et al., 2013; Shojima et al., 2004; Xiang et al., 2011a, 2013). Recent studies show that hemodynamics are promising metrics to directly impact the clinical practice on treating aneurysms (Cebral et al., 2011; Xiang et al., 2011a, 2013). Two hemodynamic parameters, wall shear stress (WSS, the tangential frictional stress caused by the action of flowing blood on the vessel wall endothelium) and oscillatory shear index (OSI, the WSS direction change during one cardiac cycle), have received particular attention due to their ability to elicit biological responses of the arterial wall (Meng et al., 2013; Shojima et al., 2004; Xiang et al., 2011a). In our previous study, we have found that low WSS and high OSI are independently associated with aneurysm rupture (Xiang et al., 2011a). This finding was corroborated by several other aneurysm hemodynamics studies (Kawaguchi et al., 2012; Lu et al., 2011; Miura et al., 2013; Zhang et al., 2011). However, a few studies have also reported high WSS to be correlated with aneurysm growth and rupture status (Castro et al., 2009; Cebral et al., 2011; Sugiyama et al., 2012).

In a recent AJNR editorial, Kallmes raised concerns on the conflicting findings and CFD modeling and assumptions (Kallmes, 2012), which has spurned a debate (Cebral and Meng, 2012; Robertson and Watton, 2012; Strother and Jiang, 2012). It has recently been proposed that both low and high WSS can elicit pathological remodeling of IAs, via different biological pathways

* Correspondence to: Department of Mechanical and Aerospace Engineering, University at Buffalo, State University of New York, Buffalo, NY 14260, USA. Tel.: +1 716 829 5406; fax: +1 716 854 1850.
E-mail address: huimeng@buffalo.edu (H. Meng).

http://dx.doi.org/10.1016/j.jbiomech.2014.09.034
0021-9290/

(Meng et al., 2013). On the other hand, it is unclear if such discrepancies could also be caused by population bias, or differences in assumptions or simplifications in CFD simulations (Cebral and Meng, 2012).

One such assumption is the inlet boundary condition. Because patient-specific inlet flow and velocity waveform is not routinely obtained, assumptions have to be made regarding CFD boundary conditions. Ideally both patient-specific aneurysm 3D geometries and patient-specific boundary conditions are required for accurate CFD simulation of aneurysms, and most image-based CFD studies are able to adopt patient-specific aneurysm geometries. While patient-specific 3D aneurysm geometries can be reconstructed from a variety of routine imaging modalities including 3D digital subtraction angiography, computed tomography angiography, and magnetic resonance (MR) angiography, patient-specific inlet boundary conditions (for flow rate and waveform) are not available from these imaging modalities. Phase-contrast MR (PC-MR) imaging or transcranial Doppler (TCD) ultrasound would be required for inlet flow measurement, but such procedures are not normally justifiable as a part of the clinical routine. Although a few CFD studies applied patient-specific boundary conditions in their simulations, these studies involved small cohorts (Boussel et al., 2008; Hassan et al., 2004; Jou et al., 2003; Sugiyama et al., 2012). The vast majority of image-based CFD studies have to adopt flow rates and waveforms measured from normal subjects or typical waveforms averaged from multiple subjects as inlet boundary conditions (Cebral et al., 2005b; Jou et al., 2008; Shojima et al., 2004; Xiang et al., 2011a). This raises important questions: What are the effects of the inlet waveform on computational hemodynamics of IAs? How might this affect aneurysm rupture risk prediction based on hemodynamic factors? The objective of this study was to examine the sensitivity of widely used hemodynamic factors derived from CFD to different inlet waveforms under the same inflow rate. We specifically focus on WSS and OSI, the two independent parameters predictive of rupture in our multivariate logistic regression model (Xiang et al., 2011a).

2. Method

Four typical internal carotid artery (ICA) aneurysms were analyzed in this study (Aneurysms (A), (B), (C) and (D) in Fig. 1). Aneurysm A (unruptured, in a 68-year-old woman) was a sidewall aneurysm with a quasi-spherical shape; Aneurysm B (unruptured, in a 66-year-old man) was a near-spherical bifurcation aneurysm with a daughter aneurysm; Aneurysm C (ruptured, in a 45-year-old woman) was a sidewall aneurysm with an irregular oblong shape and a daughter sac; and Aneurysm D (unruptured with headache symptom, in a 56-year-old woman) was a giant aneurysm on the ICA trunk. Three-dimensional angiography images of the patients' aneurysms were obtained with a Toshiba Infinix VFi/BP frontal C-arm system (Toshiba America Medical Systems, Inc., Tustin, CA). Three-dimensional images of the ICA were then reconstructed in surface-triangulation format using in-house software based on the open-source Visualization Tool Kit libraries, as previously described (Dhar et al., 2008).

Four different inlet boundary waveforms were used in flow simulations for each aneurysm (Waveforms (1)–(4) in Fig. 2). Waveform 1 was a typical ICA waveform from 17 healthy young, normal volunteers (Ford et al., 2005); Waveform 2 was a typical ICA waveform from 94 older adults (Hoi et al., 2010); Waveform 3 was an ICA waveform from a normal subject (Xiang et al., 2011a); Waveform 4 was an ICA waveform from a 56-year-old female patient with an ICA aneurysm. In order to compare the effect by different shapes of the waveforms, the same ICA mean flow rate was used for each aneurysm in the flow simulation. Additionally, steady-state simulation for each aneurysm was performed in order to compare with time-averaged WSS from the corresponding pulsatile simulations. Thus, 20 CFD simulations were performed in total.

Unstructured volumetric meshes were created using the octree approach in ICEM CFD (ANSYS, Inc., Canonsburg, PA). Finite-volume meshes consisted of tetrahedral elements with the maximum size of 0.3 mm and three prism layers with a total height of 0.1 mm near the wall for accurate calculation of WSS. The total numbers of elements ranged from 0.5 to 1 million elements in different aneurysm models. The mesh setup was based on a grid refinement study, where we tested grid sizes of 0.6 to 0.2 mm for the time-averaged velocity and pressure at centerline, and aneurysm-averaged WSS and OSI with the convergence of less than 5%. Using the CFD solver Star-CD (CD Adapco, Melville, NY) with SIMPLE solution method, we solved the flow-governing Navier–Stokes equations with second-order accuracy in space and first-order accuracy in time under pulsatile flow conditions. For spatial resolution, the liner upwind differencing scheme was applied to solve the momentum equations, while the center differencing scheme was applied to solve the mass conservation equation. For temporal resolution, Euler implicit temporal discretization was used. The Algebraic Multigrid method was used to solve the system of equations. In all simulations, a typical ICA flow rate of 4.6 mL/s from the literature (Fahrig et al., 1999) was used as inlet mean flow rate at the inlet of each model, from which the inlet mean velocity is obtained by dividing it with the inlet area. The four aforementioned velocity waveforms were scaled to this mean velocity. Traction-free boundary conditions were implemented at the outlets. When multiple outlets were present, the mass flow rate through each outlet artery was made proportional to the cube of its diameter based on the principle of optimal work (Oka and Nakai, 1987). Justified in large vessels (Lee and Steinman, 2007), blood was modeled as a Newtonian fluid and laminar flow, with a density of 1056 kg/m^3 and a viscosity of 0.0035 N s/m^2. A time step of 1 ms was used, which gave 1000 time steps per cardiac cycle. Pulsatile flow simulations were run for three cardiac cycles to ensure that numerical stability had been reached, and the solutions were saved at every 0.02 s of the last cycle for post-processing. A steady-state simulation was also performed for each aneurysm under the inlet flow rate of 4.6 mL/s (equal to the mean flow rate at the inlet in all pulsatile simulations).

We used both qualitative (contour distribution) and quantitative WSS and OSI representations over the last cardiac cycle to test their sensitivity to the inlet boundary condition. The instantaneous WSS at any point in space is time-averaged over a cardiac cycle. For quantitative comparisons of results from different waveforms, we further spatially averaged WSS and OSI over the aneurysm sac (Xiang et al., 2011a) to give the aneurysm-averaged WSS and OSI. Other hemodynamic parameters we analyzed include maximal WSS (MWSS) (Cebral et al., 2011), energy loss (EL) (Qian et al., 2011) and pressure loss coefficient (PLc) (Takao et al., 2012). These have been reported to be associated with IA rupture in studies from other groups.

3. Results

Fig. 3 shows the luminal distributions of time-averaged WSS predicted by the four pulsatile simulations with different inlet

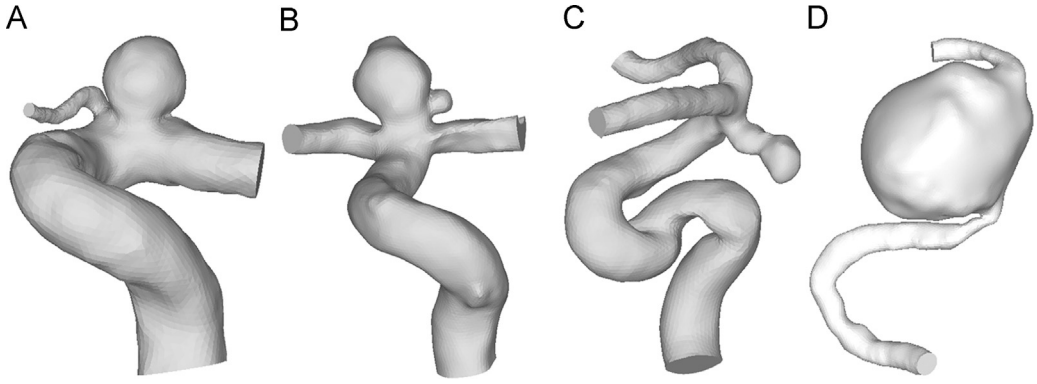

Fig. 1. Four patient-specific ICA aneurysm models for current study: Aneurysm A, a sidewall aneurysm with a quasi-spherical shape; Aneurysm B, a near-spherical bifurcation aneurysm with a daughter aneurysm; Aneurysm C, a sidewall aneurysm with an irregular oblong shape and a daughter sac and Aneurysm D, a giant, sidewall aneurysm.